Particle Structures in Elementary Cellular Automaton Rule 146

Paul-Jean Letourneau

Wolfram Research, Inc.
100 Trade Center Drive
Champaign, IL 61820, USA
paul-jean@wolfram.com

Stochastic particle-like persistent structures are found in the class 3 elementary cellular automaton rule number 146. These particles arise as boundaries separating regions with black cells occupying sites at space-time points (x, t) of constant parity $x \oplus t$. The particles execute random walks and annihilate in pairs, with particle density decaying with time in a power-law fashion. It is shown that the evolution of rule 146 closely resembles that of the additive rule 90, with persistent localized structures.

1. Elementary Cellular Automata

An elementary cellular automaton (ECA) consists of a line of cells at discrete sites x, updated in time according to a simple deterministic rule. On time step t, the color $a(x, t)$ of the cell at position x is updated to produce $a(x, t+1)$. An ECA rule F acts on the 3-cell neighborhood consisting of the cell $a(x, t)$ and its immediate left and right neighbors:

$$a(x, t+1) = F[a(x-1, t), a(x, t), a(x+1, t)]. \tag{1}$$

Here a fixed number of sites is assumed (N), with periodic boundary conditions, such that

$$x \in \{1, 2, 3, \ldots, N\}$$
$$a(N, t) = F[a(N-1, t), a(N, t), a(1, t)]$$
$$a(1, t) = F[a(N, t), a(1, t), a(2, t)].$$

That is, the right neighbor of the rightmost cell at $x = N$ is taken to be the leftmost cell at $x = 1$, and similarly the left neighbor of the leftmost cell at $x = 1$ is taken to be the rightmost cell at $x = N$ (i.e., cells arranged on a ring). We consider only elementary rules with binary-valued cells $a(x, t) \in \{0, 1\}$.

The ECA rule F is conveniently summarized in a rule table specifying the updated color of cell $a(x, t)$ for each of the $2^3 = 8$ possible configurations of the 3-cell neighborhood $\{a(x-1, t), a(x, t), a(x+1, t)\}$. Figure 1 shows the rule table for ECA rule 30.

https://doi.org/10.25088/ComplexSystems.19.2.143

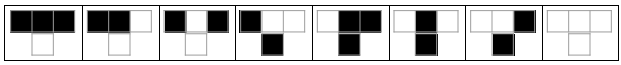

Figure 1. Rule table for ECA rule 30.

Starting with a line of N cells and a particular choice of color for each cell (the initial condition), applying the rule F in equation (1) to $a(x, t)$ for all $x \in \{1, 2, 3, \ldots, N\}$ in parallel yields an updated configuration on the next time step:

$$\mathbf{a}(t + 1) = F(\mathbf{a}(t)).$$

The resulting evolution is visualized by stacking successive $\mathbf{a}(t)$ with time t running down the page. Figure 2 shows the evolution of rule 30 for two types of initial conditions. On the left, the initial condition consists of a single black cell on a white background, corresponding to underlying site values $\mathbf{a}(0) = \{\ldots, 0, 1, 0, \ldots\}$, that is, $a(x, t = 0) = 1$ for $x = \lfloor N/2 \rfloor$ and $a(x, 0) = 0$ otherwise. This is the simplest nontrivial initial condition for an ECA, and we hereafter refer to it colloquially as "simple". On the right, the initial condition consists of N cells where the value of the cell at position x is chosen to be 1 with probability $P(x \mid a(x, 0) = 1) = 0.5$. This random initial condition has density $\rho_N \approx 0.5$, which approaches the ideal density of 0.5 in the limit of infinite system size: $\lim_{N\to\infty} \rho_N = 0.5$.

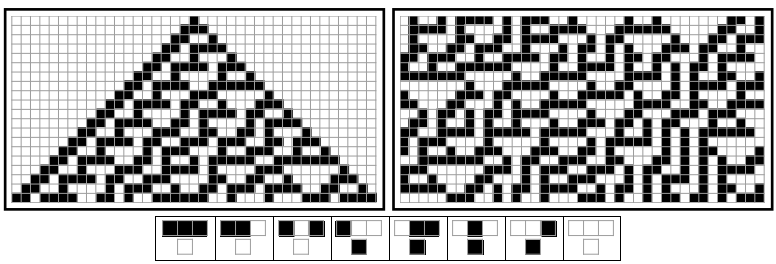

Figure 2. Evolution of ECA rule 30 from a simple (left) and random (right) initial condition. Rule table for rule 30 (bottom).

2. Rule 146

Figure 3 shows the evolution of ECA rule number 146 from simple and random initial conditions, along with the rule table. From a simple initial condition, a nested pattern is produced, identical to the evolution of rule 90 from this initial condition. Figure 4 compares the evolutions of rules 146 and 90 from simple and random initial conditions, showing that from random initial conditions the rules have different detailed behavior.

https://doi.org/10.25088/ComplexSystems.19.2.143

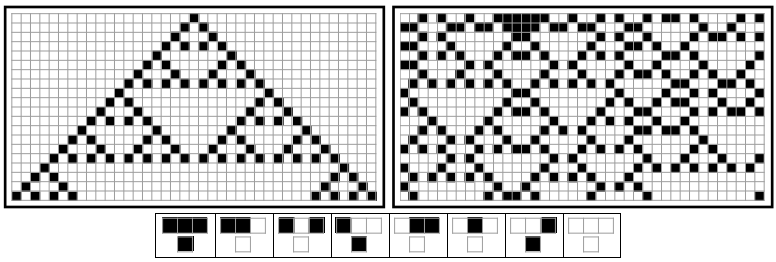

Figure 3. Evolution of ECA rule 146 from a simple (left) and random (right) initial condition. Rule table for rule 146 (bottom).

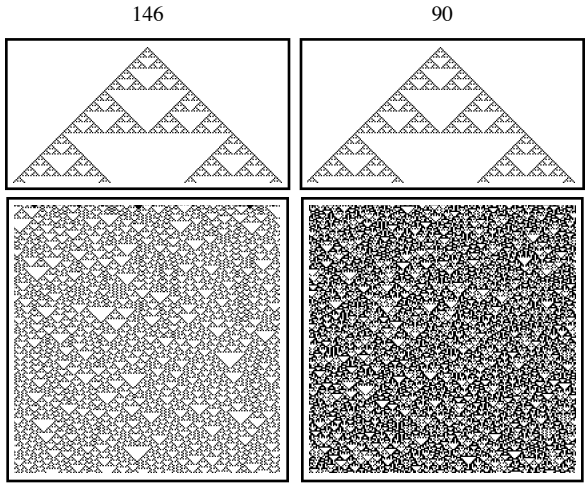

Figure 4. Evolutions of ECA rules 146 (left) and 90 (right) from simple and random initial conditions. The same random initial condition is used for both rules.

It is worth trying to understand the similarities between rules 146 and 90, since much is known about rule 90. In particular, rule 90 is additive, or linear. Additivity implies that the evolution from initial condition $\mathbf{c}(0) = \mathbf{a}(0) \oplus \mathbf{b}(0)$ satisfies

$$F[\mathbf{c}(0)] = F[\mathbf{a}(0) \oplus \mathbf{b}(0)] = F[\mathbf{a}(0)] \oplus F[\mathbf{b}(0)]$$

where $\oplus$ denotes addition modulo 2. The property of additivity makes it possible to derive a closed-form expression for the value of site $a(x, t)$ for arbitrary coordinates (x, t) without running the rule itself (reducibility) [1]. The similarity of rule 146 to rule 90 may therefore provide valuable insight into the analysis of rule 146.

Figure 5 shows a comparison of the rule tables for 146 and 90. Differences between the rule tables are limited to the three cases with in-

https://doi.org/10.25088/ComplexSystems.19.2.143

puts (1, 1, 1), (1, 1, 0), and (0, 1, 1). The rule tables are identical for the five remaining inputs: (1, 0, 1), (1, 0, 0), (0, 1, 0), (0, 0, 1), and (0, 0, 0). Note that the three inputs yielding differences are exactly those that contain adjacent black cells.

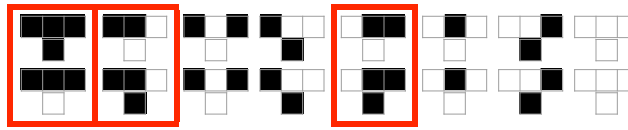

Figure 5. Comparison of rule tables for ECA rules 146 (top) and 90 (bottom).

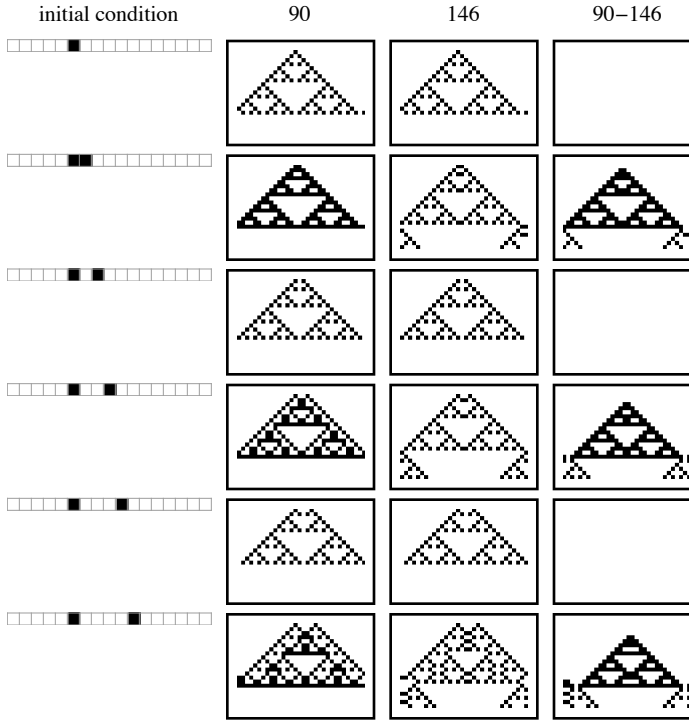

Figure 6. Evolutions of rules 90 and 146 for initial conditions where black cells are separated by an increasing number of white cells. The columns show, from left to right, the initial condition used, the evolution of rule 90, the evolution of rule 146, and the difference between the evolutions of rules 90 and 146.

Figure 6 shows the differences between evolutions of rules 90 and 146 from initial conditions of the form $\{\ldots, 0, 1, 0_n, 1, 0, \ldots\}$, with $n = 0, 1, 2, 3, 4$, that is, two black cells separated by an increasing number of white cells. Since the pattern from each point source grows

https://doi.org/10.25088/ComplexSystems.19.2.143

outward with speed 1 (i.e., one cell to the left or right per time step), they collide in the middle after about $n/2$ time steps. In particular, with n even, adjacent black cells are produced after $n/2$ steps, giving rise to a nonzero difference in the evolutions of rules 90 and 146. This difference in evolutions for even point source separations n is just what we expect given that the rule tables differ for inputs involving adjacent black cells. Furthermore, as can be seen in Figure 6, the evolutions are identical for odd n, since adjacent black cells are never generated, and only those parts of the rule tables for which the rules give identical outputs are ever exercised.

Letting $T_n(x, t)$ denote the appearance of the pattern $\{0, 1, 0_n, 1, 0\}$ on time step t centered at position x, we may summarize our analysis by saying that the presence of the substructure $T_{2n}(x, t)$ with $n = 1, 2, 3, \ldots$ is a sufficient condition for the evolution of rule 146 to diverge from that of rule 90. That is, for $\mathbf{a}_{T_{2n}}(t) = \{\ldots, T_{2n}(x, t), \ldots\}$,

$$F_{90}^{n+1}\left[\mathbf{a}_{T_{2n}}(t)\right] \neq F_{146}^{n+1}\left[\mathbf{a}_{T_{2n}}(t)\right] \tag{2}$$

where F^{n+1} denotes $n+1$ iterations of F.

3. Persistent Structures in Rule 146

Having identified the cases in which rule 146 differs from rule 90, it seems sensible to try to highlight the portions of the evolution wherein 146 diverges from 90. This can be thought of as a sort of linearity analysis, viewing the evolution of 146 as a slight deviation from the purely additive behavior of rule 90.

Figure 7 shows an evolution of rule 146 with all occurrences of the substructure $T_{2n}(x, t)$ highlighted for $n = 0, 1, 2, \ldots$. It is immediately clear that this structure persists in time and remains spatially localized.

As noted earlier, even runs of white cells $T_{2n}(x, t)$ would generate a pair of adjacent black cells $T_0(x, t)$ after n steps via the processes

$$F_{146}[\{\ldots, T_{2n}(x, t), \ldots\}] \to \{\ldots, T_{2(n-1)}(x, t+1), \ldots\} \tag{3}$$

$$F_{146}^{(n)}[\{\ldots, T_{2n}(x, t), \ldots\}] \to \{\ldots, T_0(x, t+n), \ldots\}. \tag{4}$$

Figure 7 shows an additional process in rule 146 that occurs as a result of the local environment of the persistent structure. In the following process, pairs of adjacent black cells $T_0(x, t+n)$ at the base of triangle $T_{2n}(x, t)$ nucleate another even triangle T_{2m} on the next step:

$$\begin{aligned} &F_{146}\left[\{\ldots, T_0(x, t+n), \ldots\}\right] \to \\ &\quad \{\ldots, T_{2m}(y, t+n+1), \ldots\}. \end{aligned} \tag{5}$$

https://doi.org/10.25088/ComplexSystems.19.2.143

Process (5) can be seen taking place in Figure 7, where adjacent black cells appear at the base of every (highlighted) triangle containing even runs of white cells. It is not immediately clear whether the size of successive even triangles $2n$ and $2m$ are in any way correlated, or whether the respective positions x and y are correlated.

The overall process after $n+1$ steps is given by combining the "triangle-pair" process (4) and "pair-triangle" process (5):

$$F_{146}^{(n+1)}[\{\ldots, T_{2n}(x, t), \ldots\}] \rightarrow \{\ldots, T_{2m}(y, t+n+1), \ldots\}. \tag{6}$$

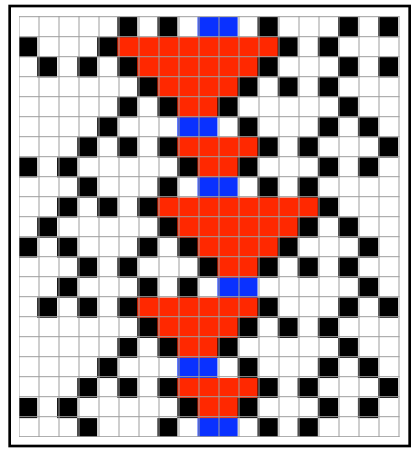

Figure 7. Evolution of rule 146 with two types of substructure highlighted: adjacent black cells (in blue/dark gray), and even runs of white cells (in red/light gray). The width-10 initial condition used contains a single pair of adjacent black cells in the center, and only odd runs of white cells with no other adjacent black cells everywhere else.

Figure 8 shows a larger, width-100 evolution of rule 146, with an initial condition containing a single instance of $T_{2n}(x, 0)$, with $T_{2n}(x, t)$ highlighted in the same way as in Figure 7. The persistent structure formed by successive iterations of the process (6) appears to do something like a random walk. Figure 9 shows the appearance of many such structures when starting from a random initial condition. It is immediately apparent from Figure 9 that the persistent structures tend to annihilate in pairs. The conditions for such annihilations, however, look to be highly dependent on the details of the local environment.

https://doi.org/10.25088/ComplexSystems.19.2.143

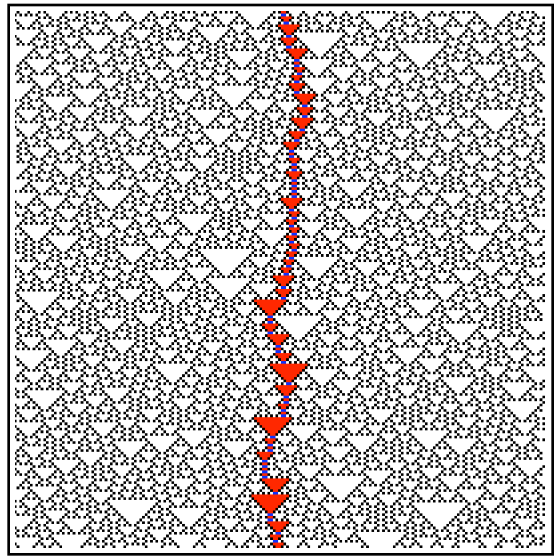

Figure 8. A larger evolution of rule 146 from an initial condition with a single even run of white cells in the center, with the resulting persistent structure highlighted in the same way as in Figure 7.

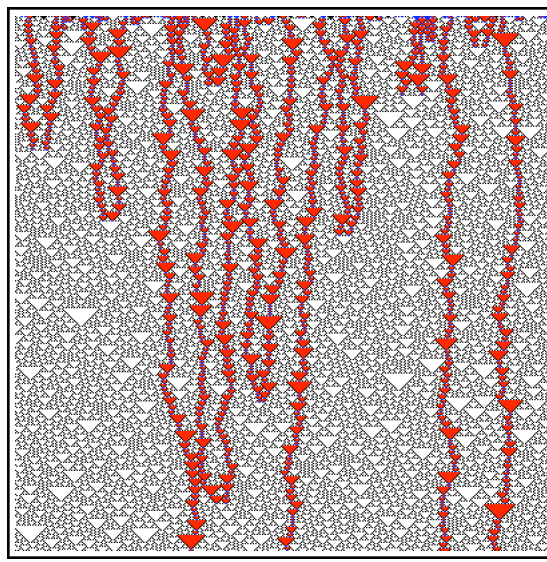

Figure 9. The evolution of rule 146, starting from a random initial condition, with persistent structures highlighted in the same fashion as in Figure 7.

https://doi.org/10.25088/ComplexSystems.19.2.143

4. Analysis of Persistent Structures

Since the persistent structures in Figure 9 constitute all occurrences of even runs of white cells $T_{2n}(x, t)$ (including pairs of black cells $T_0(x, t)$ for $n = 0$), the regions between structures contain only odd runs $T_{(2n+1)}(x, t)$ of white cells separated by isolated black cells. For a given time step t, this implies that black cells occupy either even sites $x \oplus 2 = 0$ or odd-numbered sites $x \oplus 2 = 1$, but not both.

Furthermore, as shown in Section 2, even runs $T_{2n}(x, t)$ are entirely responsible for differences in evolution between rules 146 and 90 (cf. equation (2)). Since the regions between persistent structures lack any occurrences of $T_{2n}(x, t)$ (by definition), these regions evolve locally according to rule 90.

It is easy to see that rule 90 is *parity-preserving*. That is, given a configuration $\mathbf{a}_0(t)$ containing black cells only on sites with $x \oplus t = 0$ (*even parity*), on the next time step rule 90 generates black cells only on sites satisfying $x \oplus (t + 1) = 0$ (this follows from the fact that the rule 90 rule table is independent of the center site):

$$F_{90}\left[\mathbf{a}_0(t)\right] \rightarrow \mathbf{a}_0(t + 1).$$

The same is true for odd parity. Therefore, we conclude that regions between persistent structures are of a single parity.

Since the persistent structures always contain an even number of cells, it is easily seen that the parity of black-occupied sites must change as one crosses over a structure. That is, the persistent structures represent a *boundary* between regions of different parities. We can think of these regions of different parities as having different *phases*, and the boundaries separating them as *phase boundaries*.

Figure 10 shows this idea of phases for rule 90. The evolution at the top is split into two lattices with opposite parities, even ($x \oplus t = 0$) and odd ($x \oplus t = 1$). The resulting evolutions are precisely that of the ECA rule 60, which has the same rule table as rule 90 if the middle and rightmost cells are transposed in each 3-cell neighborhood of the rule table.

Figure 11 shows the same phase separation for rule 146. The resulting evolutions show regions of a single parity (evolving locally according to rule 60), separated by white space where an opposite-parity region intervened. The jagged boundaries of the single-parity regions are precisely the persistent structures seen when one highlights even runs in the evolution of rule 146.

It is interesting to note that for rule 90 the two phases in Figure 10 evolve independently on adjacent lattice sites, while rule 146 actively separates these two phases into spatially distinct regions, separated by phase boundaries. These phase boundaries have the behavior of stochastic particles, the statistical properties of which are the subject of Section 5.

https://doi.org/10.25088/ComplexSystems.19.2.143

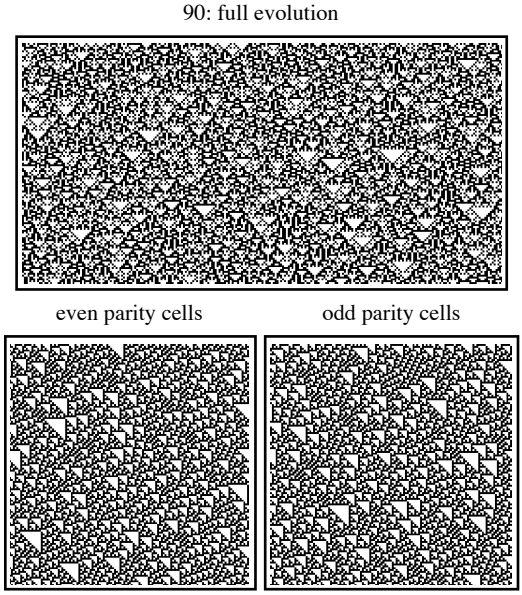

Figure 10. Separating the evolution of rule 90 (top) into two phases: cells with even parity (bottom left) and cells with odd parity (bottom right).

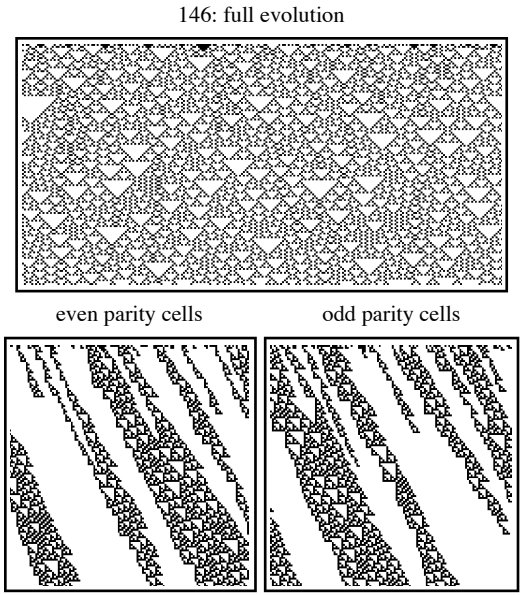

Figure 11. Separating the evolution of rule 146 (top) into two phases, as was done for rule 90 in Figure 10: cells with even parity (bottom left) and cells wit odd parity (bottom right).

https://doi.org/10.25088/ComplexSystems.19.2.143

When the evolution of rule 146 is perturbed by a point-change in the initial condition, the trajectories of the phase boundaries are affected. Figure 12 shows the evolutions of rules 146 and 90 from initial conditions differing in only a single site in the middle. The difference pattern of rule 90 is simply the evolution from the initial difference, which follows trivially from additivity. Rule 146 shows a combination of linear and nonlinear parts in the perturbation. Figure 13 shows the perturbed trajectories of the phase boundaries superimposed on the perturbation pattern. It is clear that the nonlinear portion of the perturbation follows the phase boundaries. This is due to the fact that the deflection of the phase boundary by the perturbation leaves a region occupied by both lattice parities in the difference pattern.

The character of perturbations in rule 146 is reminiscent of light and particles. The linear portion of the perturbation travels at light speed, while the nonlinear portion travels at a speed governed by the speed of the "particles" in the system (the phase boundaries). More concrete analogies may be drawn with classical particles by considering the perturbation as a one-dimensional Green's function for the system [2].

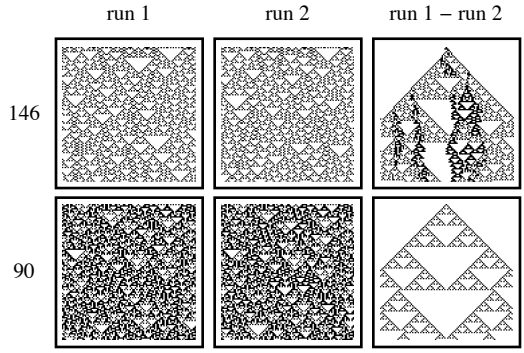

Figure 12. Evolutions of rules 146 and 90 from initial conditions differing in only a single site in the middle. The difference between the two evolutions is shown on the right. Due to the additivity of rule 90, the difference in evolutions is simply the evolution from the initial difference. Rule 146 shows a more complex difference pattern, with both a linear (90-like) portion and a nonlinear portion. The nonlinear portion arises from the deflection of phase boundaries within the light cone of the perturbation event.

https://doi.org/10.25088/ComplexSystems.19.2.143

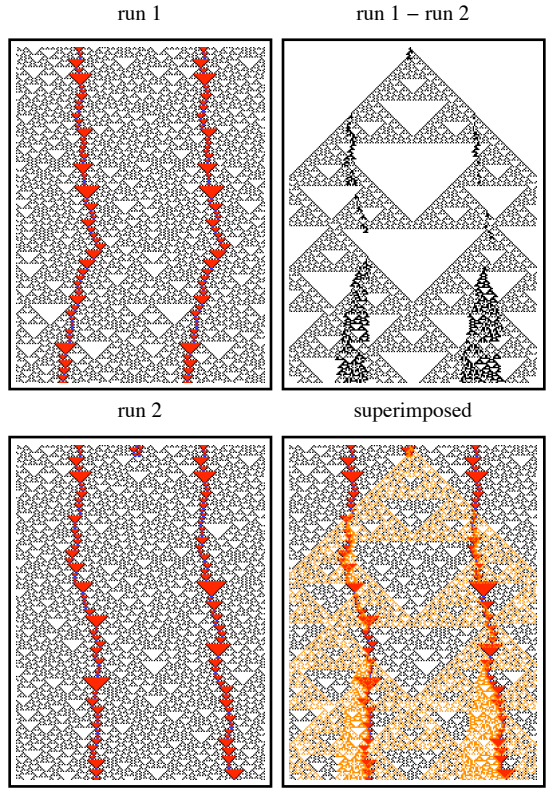

Figure 13. Perturbed evolution of rule 146, showing the deflection of phase boundaries in the light cone of the perturbation event in the initial condition. In the bottom right image, the perturbed trajectories of the phase boundaries are shown superimposed on the difference pattern.

5. Statistical Properties

The evolution of rule 146 from a random initial condition, shown in Figure 4, gives little indication that even-width triangles $T_{2n}(x, t)$ behave somehow differently than odd-width triangles $T_{2n+1}(x, t)$. However, the particle-like behavior of the even triangles becomes apparent when the substructures $T_{2n}(x, t)$ are highlighted, as in Figure 7. This is in sharp contrast to class 4 behaviors, such as rule 110, where persistent structures and their complex interactions are readily visible. Wolfram's Principle of Computational Equivalence makes the claim that class 3 rules should in fact be universal [3]. Finding and analyzing persistent structures in class 3 rules is one way to go about discovering how information is propagated in these systems.

https://doi.org/10.25088/ComplexSystems.19.2.143

Does statistical analysis give any indication that these even-width triangles play a different role in the system than the odd triangles?

Figure 14 shows the distribution of run lengths in the evolution of rule 146 from a random initial condition. Here a "run" of white cells is defined as a substructure of the form $\{.., 1, 0_n, 1, ...\}$, and $\{.., 0, 1_n, 0, ...\}$ for a run of black cells. The plot shows (on a log scale) the frequency of run lengths P_n for a single simulation of 1000 steps from a random initial condition of width 10 000. Note that the vast majority of run lengths above $n = 2$ are contributed by white runs, since longer black runs decay quickly away from the initial condition in a short initial transient, and are never subsequently generated. The distribution of even and odd run lengths are both well fit to an exponential $P_n \sim \exp(-\beta n)$, but clearly have a statistically significant difference in decay constants β, with $\beta_{2\,n} = 0.304 \pm 0.004$ and $\beta_{2\,n+1} = 0.359 \pm 0.002$. Therefore, the statistical distribution of run lengths alone gives an indication of the special role played by even-run triangles in rule 146.

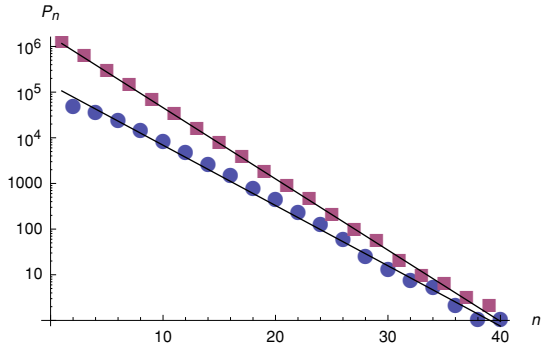

Figure 14. Frequency of run lengths P_n for a single simulation of 1000 steps from a random initial condition of width 10 000, where runs of white and black cells are substructures of the form $\{.., 1, 0_n, 1, ...\}$ and $\{.., 0, 1_n, 0, ...\}$, respectively. The distribution of even and odd run lengths are both well fit to an exponential $P_n \sim \exp(-\beta n)$, but with different decay constants $\beta_{2\,n} = 0.304 \pm 0.004$ and $\beta_{2\,n+1} = 0.359 \pm 0.002$.

In Section 3, we questioned the nature of the correlations between positions x and y of successive triangles $T_{2\,n}(x, t)$ and $T_{2\,n}(y, t)$ along the phase boundary (in process (5)). Figure 15 shows the mean-square displacement $\langle x^2 \rangle$ of the phase boundaries from their starting position as a function of the number of time steps t. The data shown is based on an average over 100 simulations with only a single structure present (as in Figure 8). While there are large fluctuations, the data is plausibly linear, that is, $\langle x^2 \rangle \sim t$. This indicates the structures are doing essentially a random walk.

https://doi.org/10.25088/ComplexSystems.19.2.143

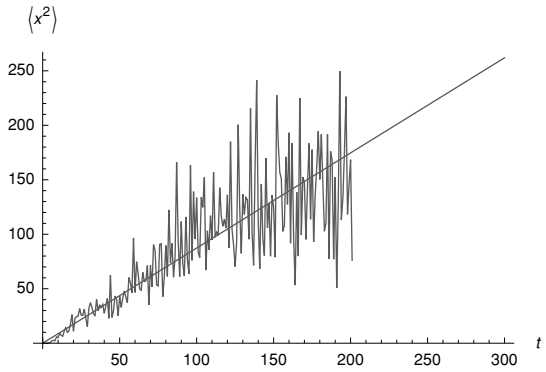

Figure 15. Mean-square displacement of persistent structures from their starting position as a function of time t.

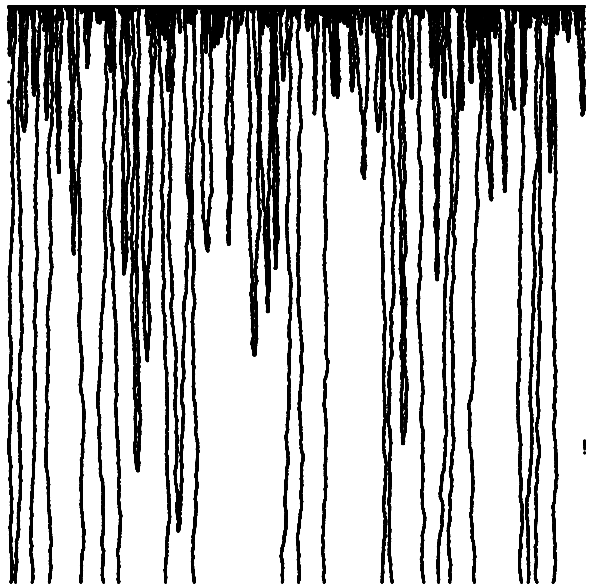

Figure 16. Large-scale view of the evolution of rule 146 from a random initial condition of width 10 000, run for 10 000 steps, showing only the paths of the persistent structures highlighted in Figures 7 through 9. Each point represents the midpoint of an even run of white cells 0_{2n}.

A large-scale view of the evolution of rule 146 is provided in Figure 16. Here, only the paths of the phase boundaries $T_{2n}(x, t)$ are shown by placing a dot at spacetime points (x, t) at the midpoint of the triangle. The pairwise annihilation of structures seen previously in

https://doi.org/10.25088/ComplexSystems.19.2.143

Figure 9 is also readily apparent at this scale. Figure 17 shows the density $n_b(t)$ of phase boundaries as a function of time t. The density is a power-law of the form

$$n_b(t) \sim t^{-\alpha}$$

with $\alpha = 0.4789 \pm 0.0006$. Note that this is not consistent with a purely diffusive pairwise annihilation of structures, for which one would expect $\alpha = 1/2$ [4]. Note that qualitatively similar results are obtained for rules 18, 122, 126, 146, and 182 [4].

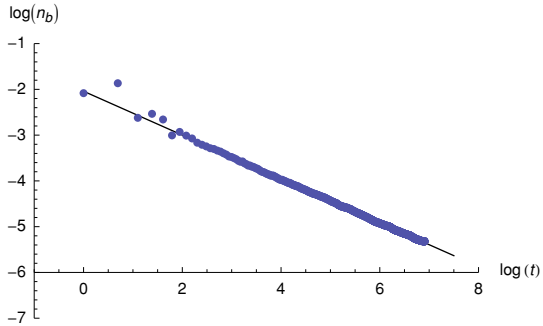

Figure 17. Density $n_b(t)$ of pairs of black cells as a function of time t. Note the natural logarithm $\log n_b(t)$ is plotted against log time $\log t$. The linearity of the data on a log-log scale implies a power-law. The superimposed line shows a fit of the form $n_b(t) = C\,t^{-\alpha}$ with a least-squares fit giving $\alpha = -0.4789 \pm 0.0006$ and $\alpha \log C = -2.041 \pm 0.003$. The system width N here is 60 000, with normalization based on 30 000 possible pairs on a given time step t. Note that points at large values of t were averaged over a sliding window in order to suppress statistical fluctuations.

References

[1] O. Martin, A. M. Odlyzko, and S. Wolfram, "Algebraic Properties of Cellular Automata," *Communications in Mathematical Physics*, **93**(2), 1984 pp. 219-258.

[2] S. Wolfram, "Universality and Complexity in Cellular Automata," *Physica D*, **10**(1-2), 1984 pp. 1-35.

[3] S. Wolfram, *A New Kind Of Science*, Champaign, IL: Wolfram Media, Inc., 2002.

[4] P. Grassberger, "Chaos and Diffusion in Deterministic Cellular Automata," *Physica D*, **10**(1-2), 1984 pp. 52-58.

https://doi.org/10.25088/ComplexSystems.19.2.143